Anomalous surfactant diffusion in a living polymer system

Ruggero Angelico,[1,4,*] Andrea Ceglie,[1,4] Ulf Olsson,[2] Gerardo Palazzo,[3,4] and Luigi Ambrosone[1,4,†]
[1]*Università del Molise, DISTAAM, Via De Sanctis, I-86100 Campobasso, Italy*
[2]*Physical Chemistry 1, Center for Chemistry and Chemical Engineering, Lund University, P.O. Box 124, SE-221 00 Lund, Sweden*
[3]*Dipartimento di Chimica, Università di Bari, Via Orabona 4, I-70126 Bari, Italy*
[4]*Consorzio Interuniversitario per lo sviluppo dei Sistemi a Grande Interfase (CSGI), Florence. Italy*
(Received 5 June 2006; published 20 September 2006)

Random processes are generally described by Gaussian statistics as formulated by the central limit theorem. However, there exists a large number of exceptions to this rule that can be found in a variety of fields. Diffusion processes are often analyzed by the scaling law $\langle r^2\rangle \sim t^{2\beta}$, where the second moment of the diffusion propagator or molecular mean square displacement, $\langle r^2\rangle$, in the case of Gaussian diffusion is proportional to t, i.e., $\beta=1/2$. A deviation from Gaussian behavior may be either superdiffusion ($\beta>1/2$) or subdiffusion ($\beta<1/2$). In this paper we demonstrate that all three diffusion regimes may be observed for the surfactant self-diffusion, on the length scale of 10^{-6} m and the time scale of 0.02–0.8 s. in a system of wormlike micelles, depending on small variations in the sample composition. The self-diffusion is followed by pulsed gradient NMR where one not only measures the second moment of the diffusion propagator, but actually measures the Fourier transform of the full diffusion propagator itself. A generalized diffusion equation in terms of fractional time derivatives provides a general description of all the different diffusion regimes, and where $1/\beta$ can be interpreted as a dynamic fractal dimension. Experimentally, we find $\beta=1/4$ and $3/4$, in the regimes of sub- and superdiffusion, respectively. The physical interpretation of the subdiffusion behavior is that the dominating diffusion mechanism corresponds to a lateral diffusion along the contour of the wormlike micelles. Superdiffusion is obtained near the overlap concentration where the average micellar size is smaller so that the center of mass diffusion of the micelles contributes to the transport of surfactant molecules.

DOI: 10.1103/PhysRevE.74.031403 PACS number(s): 82.70.−y, 05.40.Fb, 61.43.Hv

I. INTRODUCTION

Random processes often obey Gaussian statistics as described by the central limit theorem. However, despite the omnipresence of Brownian motion as a transport mechanism, it is known that different kinds of diffusion processes exists. Indeed, it has been found in recent years that anomalous non-Gaussian diffusion can occur in many complex systems. These range from turbulent fluids, to chaotic dynamical systems, to disordered media. In these systems, anomalous *sub*- and *super*diffusion mechanisms, closely related to normal diffusion but with some qualitatively different properties, drive the physics of the transport processes. These mechanisms of anomalous diffusion are adequate for describing various applicative problems in biology [1–3], economics [4,5], physics [6–8] and chemistry [9–13]. In particular, for some surfactant-based complex fluids, such as liquid single-phase microemulsions, experimental evidences of two subclasses of the anomalous diffusion have been found [14–16]. A micellar system for which a *sub*diffusive molecular transport has been observed is the ternary lecithin-water-cyclohexane system, whose microstructure was extensively studied in the recent years [17]. Lecithin monomers can assemble reversibly in organic solution to form various supramolecular structures of the reverse (water-in-oil) type. Reverse micelles are spherical at very low micellar (surfactant *plus* water) volume fraction Φ, but undergo uniaxial water-induced growth to become polydisperse wormlike cylindrical aggregates that can attain lengths from several hundred nanometers to micrometers as Φ and W_0, the water-to-surfactant mole ratio, are increased. A variation of W_0 at constant surfactant concentration does primarily influence the micellar contour length L (or the aggregation number). At a threshold surfactant volume fraction Φ^* (which depends on W_0 [18]) these inverted cylindrical micelles start to entangle and form a transient network, similar to semidilute polymer solutions, and they form highly viscous and non-Newtonian solutions at even moderate concentrations. At still higher concentrations, mesophases exhibiting nematic, hexagonal, or lamellar ordering have been found [19].

Thus, the special interest in this system is due to the many similarities between such micellar solutions and classical polymer solutions, though the worms—sometimes called *living polymers*—break and reform continuously [20]. The present investigation provides further experimental evidence of anomalous molecular diffusion in living polymer systems and affords a widespread model deduced through the formalism of the fractional differential equations framework by which NMR self-diffusion data can be opportunely analyzed. A strong signature of anomalous subdiffusion was already reported by us in a different regime of compositions [15]. Here, we present experimental proof of a smooth transition from *super*- to *sub*type anomalous diffusion by passing through an apparent normal diffusion regime, which has never been found in microemulsion systems, to the best of our knowledge.

*Corresponding author. Email address: angelico@unimol.it
†Email address: ambroson@unimol.it

II. EXPERIMENTAL SECTION AND DATA TREATMENT

We present lecithin self-diffusion data at 25 °C in the system lecithin–water–cyclohexane-d_{12} measured along (1) a water dilution line, where W_0 has been varied in the range 4–10 at constant $\Phi=0.02$, and (2) an oil dilution line, where W_0 has been kept constant at four while Φ was varied in a narrow range of compositions, $0.02 \leqslant \Phi \leqslant 0.05$; the lower limit being just above to the entanglement threshold Φ^* where the transition from dilute (noninteracting aggregates) to the semidilute (intertwined coils) regime occurs for $W_0=4$ (Φ^* decreases with increasing W_0 [18]). Soybean lecithin (Epikuron 200) was a generous gift from Degussa Bioactives AG and consists of soybean phosphatidylcholine with a purity of 95% and with an average molecular weight of 772 [21]. The lecithin used in this work is of the same brand used in most of the published investigations of this system, and as in previous work, it was used without further purification which consequently means that it is a certain mixture of phosphatidylcholines of different chain lengths and degree of saturation [21]. To minimize the intensity from the solvent protons, micellar solutions were made with perdeuterated cyclohexane purchased from Dr. Glasel (Basel), which was used as received. Water was millipore filtered.

Pulsed field gradient spin-echo (PGSE) ^{1}H-NMR self-diffusion measurements were performed at 25 °C±0.5 on a Bruker DMX-200 spectrometer, by measuring the echo attenuations of the intensity of trimethyl ammonium, $-N(CH_3)_3$ (3.3 ppm) and terminal methyl protons $-CH_3$ (0.9 ppm) of the lecithin molecule in the spectra, obtained by Fourier transform of the second half of the echo. Data from $-CH_3$ signal were collected only after the complete decay of the signals coming from minor oil soluble impurities present in the used soybean lecithin. To monitor the molecular diffusion, the PGSE NMR technique enjoys certain advantages over others in that it is capable of measuring self-diffusion coefficients over a wide range from fast (above 10^{-9} m^2 s^{-1}) to very slow diffusion (below 10^{-14} m^2 s^{-1}), and the technique can provide individual self-diffusion coefficients from mixtures of diffusing molecules [22] without the need for artificial labeling.

For the present study, self-diffusion experiments have been performed by using the stimulated echo sequence (STI) rather than the classical Hahn echo, not only to overcome the rapid transverse relaxation of lecithin protons but also because the appearance of anomalous non-Gaussian diffusion effects. Investigating these phenomena often requires measurements with different diffusion times t, but varying t in classical spin echo experiments produces a strong dependence on the transverse relaxation time T_2. In surfactant aggregates, such as the long lecithin wormlike micelles, T_2 can be dominated by the slow overall dynamics of the micelle. Hence, varying t in classical Hahn echo pulse sequence may produce an unwanted size selection [23]. On the other hand, varying t in STI experiments provides a T_1 dependent result: since T_1 at the applied magnetic field depends only on the local dynamics, no selection on the basis of the large scale structure can be expected. Therefore STI measurements at different t should be scarcely affected by relaxation "artifacts." In simple liquids, characterized by ordinary Brownian mass transport, the attenuations of the NMR signals obeys the Stejskal-Tanner relationship [24],

$$\ln E(q,t) = -q^2 Dt, \tag{1}$$

where $E(q,t)$ is the normalized echo amplitude, $q=\gamma\delta G$, γ is the gyromagnetic ratio of the nucleus under investigation (^{1}H), δ and G the duration and the strength of the applied gradient pulse, respectively, D is the self-diffusion coefficient, and t is the time interval between two successive gradient pulses. Measurements have been carried out by varying the magnitude of G while keeping δ (typically 3 ms) and t constant during each experimental run. In order to reveal a possible anomalous diffusion behavior, the time between the first two 90° pulses in STI has been kept short and constant at 6 ms, while the time between the second and third 90° pulse varied in the range 14–794 ms, the other experimental parameters being constant for each run. Thus, all measurements have been performed in the narrow pulse approximation or *short-gradient-pulse* (SPG) limit, i.e., where motion during the duration of the gradient pulse is negligible ($\delta \ll t$). The absence of artifacts in the time-variation NMR experiments has been checked by measuring D, inside the same t interval used in this study, of a dry glycerol sample, and verifying the constancy of the self-diffusion coefficient in accord with the literature values [25]. If the process underlying the molecular diffusion is typically Gaussian, Eq. (1) predicts that the self-diffusion coefficient D can be extracted from the slopes of the attenuation profiles obtained from linear regression of $\ln E(q,t)$ as a function of q^2t, at fixed values of δ and t. Rigorous treatment (in the SPG limit) gives the following dependence of the echo on the applied gradient [24],

$$E(q,t) = \int_{-\infty}^{+\infty} P(z,t) e^{-iqz} dz, \tag{2}$$

where $P(z,t)$ is the average diffusion propagator, q is the effective wave vector defined above, and z is the direction of the observed displacement which is identical to the direction of the field gradient. One can show that $P(z,t)$ obeys the diffusion equation,

$$\frac{\partial P(z,t)}{\partial t} = D \frac{\partial^2 P(z,t)}{\partial z^2}. \tag{3}$$

Such an equation has to be solved for a given initial condition $P(z,0)$ and with suitable boundary conditions. Its typical solution is

$$P(z,t) = \frac{1}{\sqrt{4\pi Dt}} e^{-z^2/4Dt} \tag{4}$$

which describes a propagator that as time elapses is smoothed out and broadens and characterized by a mean square displacement (MSD), $\langle z^2 \rangle$, that scales linearly with t ($=2Dt$). Then the experimental echo decay, obtained from Eq. (2), assumes the usual form described in Eq. (1). When $P(z,t)$ is unknown, one can still determine the MSD by evaluating the initial slope of $E(q,t)$ when plotted as a func-

tion of q^2. Indeed, in the limit of small q, Eq. (2) is changed in

$$E(q,t)_{q\to 0} = \int_{-\infty}^{+\infty} dz P(z,t)\left[1 + iqz - \frac{(qz)^2}{2} + \cdots\right]$$

$$\approx 1 - \langle z^2\rangle \frac{q^2}{2} + \cdots . \quad (5)$$

Operatively, for each measured $E(q,t)$ the related limiting slope has been calculated from least-squares fitting of the first section of normalized decay, corresponding to 30% of full echo attenuation, with a second order polynomial function $E(q,t) \approx 1 - ax + bx^2$, where $x = q^2$ and $a = \frac{1}{2}\langle z^2\rangle$, a and b being fitting parameters.

III. THEORETICAL CONSIDERATIONS

A linear time dependence of $\langle z^2(t)\rangle$ is the hallmark of Gaussian diffusion and it is used experimentally, numerically, and theoretically to probe the molecular motion. However, our measurements display an anomalous behavior. In general terms, the MSD can be always expressed either as a smooth function of time [26,27] or as [28,29]

$$\langle z^2(t)\rangle \sim t^{2\beta}. \quad (6)$$

As it will be discussed below, β is related to the dynamic fractal dimension d_w through $\beta = d_w^{-1}$. Obviously, for $\beta = 1/2$, Eq. (6) gives $\langle z^2\rangle \sim t$ and the diffusion process can be described by a classical random walk (normal or Gaussian diffusion); for $\beta < 1/2$ the rate of growth of MSD is lower and the transport is termed *sub*diffusive, whereas for $\beta > 1/2$ the rate is higher and the mechanism of the transport is termed *super*diffusive. Equation (3) can be generalized by replacing the first-order time derivative by a fractional derivative of order 2β, according to Caputo and Mainardi [30]. In our notation it reads

$$\frac{\partial^{2\beta} P(z,t)}{\partial t^{2\beta}} = D_{2\beta} \frac{\partial^2 P(z,t)}{\partial z^2}, \quad 0 < \beta \leqslant 1, \quad (7)$$

where $D_{2\beta}$ denotes a diffusion constant with dimensions $[L^2][T^{2\beta}]$ We recall the definition of Caputo fractional derivative of order $2\beta > 0$ for a function $f(t)$,

$$\frac{d^{2\beta} f(t)}{dt^{2\beta}} = \frac{1}{\Gamma(m - 2\beta)} \int_0^t (t-\tau)^{m-2\beta-1} f^{(m)}(\tau) d\tau, \quad (8)$$

where $m = 1,2\ldots$ and $0 \leqslant m-1 < 2\beta \leqslant m$; $f^{(m)}$ denotes the mth derivative of $f(t)$. According to Eq. (8) we need to distinguish the cases $0 < \beta \leqslant \frac{1}{2}$ and $\frac{1}{2} < \beta \leqslant 1$. We note that in this latter case, Eq. (7) can be seen as a sort of interpolation between the standard diffusion equation and the classical wave equation leading to a superdiffusive ballistic motion. For the fractional diffusion equation the Fourier transformation leads to the ordinary equation of order 2β,

$$\left(\frac{d^{2\beta}}{dt^{2\beta}} + q^2 D_{2\beta}\right) E(q,t) = 0. \quad (9)$$

The application of Laplace transform through the *Caputo* formula yields the solution [30]

$$E(q,t) = E_{2\beta}(-q^2 D_{2\beta} t^{2\beta}), \quad (10)$$

where $E_{2\beta}(x)$ denotes the Mittag-Leffler function of order 2β defined by [31]

$$E_{2\beta}(x) = \sum_{n=0}^{\infty} \frac{x^n}{\Gamma(2\beta n + 1)}. \quad (11)$$

When $\beta \neq \frac{1}{2}$ the inversion of Fourier transform of Eq. (11) cannot be obtained by using the standard tables of Fourier transform pair functions; notwithstanding, for $0 < \beta \leqslant 1$ such an inversion can be achieved by turning to the Laplace transform pairs. For the time-fractional diffusion equation the fundamental solution is still a symmetric probability density function in z but is no longer of the Gaussian type. The exact solution of the propagator can be given in close form in terms of Fox functions [32].

Here we note only that there are two branches for $z > 0$ and $z < 0$, which exhibit an exponential decay. This assures that all absolute moments are finite:

$$\langle z^{2n}(t)\rangle = \int_{-\infty}^{+\infty} z^{2n} P(z,t) dz = \frac{\Gamma(2n+1)}{\Gamma(2\beta n + 1)} (D_{2\beta} t^{2\beta})^n. \quad (12)$$

Since one experimentally estimates $\langle z^2(t)\rangle$ from the limiting slope of $E(q,t)$, we have to set $n = 1$ in Eq. (12) to compare theory with experiments. We recognize that the MSD is now proportional to $D_{2\beta} t^{2\beta}$, which for $\beta \neq 1/2$ implies the phenomenon of anomalous diffusion.

IV. RESULTS

A. Water dilution line, $W_0 = 4-10$ at fixed $\Phi = 0.02$

First, we briefly summarize our self-diffusion results reported for the lecithin water C_6D_{12} system in the narrow composition range $\Phi = 0.02-0.05$ and $W_0 = 4-10$. Figure 1 shows semilog plots of the experimental surfactant echo decays $E(q,t)$ vs $q^2 t$ along the explored water dilution line. Evident departures from normal Gaussian behavior are (a) deviations from linearity and (b) that the echo decays depend on t as a function of $q^2 t$. The former feature is almost conserved in all the measured $E(q,t)$ while the latter reveals a very peculiar trend varying from an apparent *increase* of the limiting slope (for $q \to 0$) with increasing t, displayed in Fig. 1(a) ($W_0 = 4$, $t = 20-800$ ms) and Fig. 1(b) ($W_0 = 6$, $t > 100$ ms), followed by independence of time scale in Fig. 1(b) ($W_0 = 6$, $t = 20-100$ ms) and Fig. 1(c) ($W_0 = 8$, $t = 20-800$ ms) with all echoes superimposed, and finally the trend is inverted in Fig. 1(d) for $W_0 = 10$, characterized by a *decrease* of the slope with increasing the experimental time t.

In order to determine β from each $E(q,t)$ curve of Figs. 1(a)–1(d), the $\langle z^2(t)\rangle$ has been extracted using Eq. (5) and plotted vs *time* in a log-log plot (Fig. 2). For the lowest water content ($W_0 = 4$), the superdiffusive scaling parameter, $\beta = 3/4$, is obtained in the whole time interval $200 < t < 800$ ms; at intermediate value, $W_0 = 6$, superdiffusive behavior appears above t^* (with $t^* \approx 200$ ms). An apparent Gaussian coefficient, $\beta = \frac{1}{2}$, is obtained for $W_0 = 8$ in the whole t range explored and a subdiffusive regime is encoun-

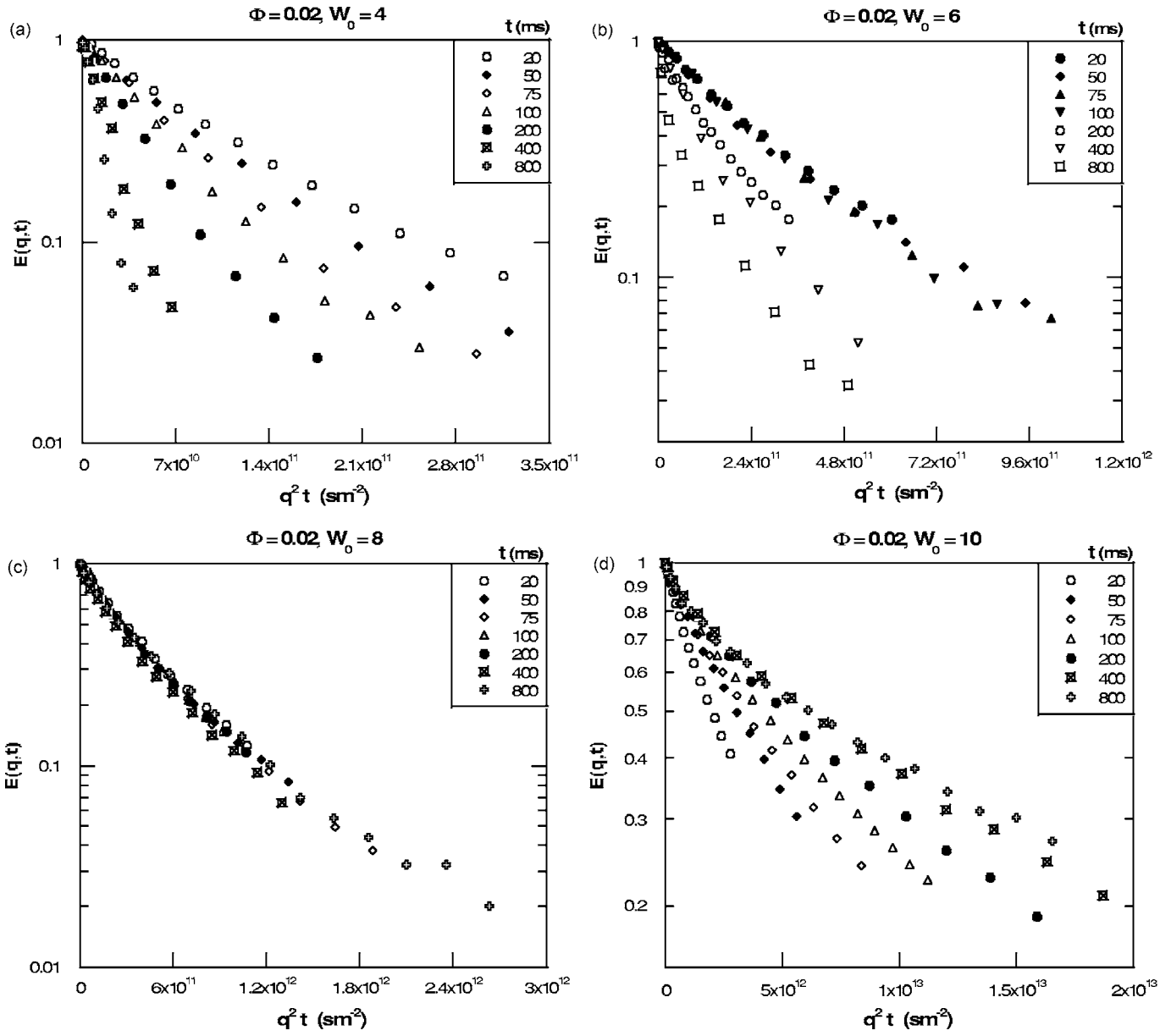

FIG. 1. Semilogarithmic plots of normalized lecithin echo attenuations $E(q,t)$ for $t=20-800$ ms, as a function of q^2t at different water to lecithin molar ratio $W_0=4-10$ and constant micellar volume fractions $\Phi=0.02$. (a) $W_0=4$, nonexponential decays whose slopes increase with t indicating superdiffusive behavior; (b) $W_0=6$, here echoes in the time window $20<t<100$ ms overlap while at higher t slopes increase with time; (c) $W_0=8$, deviations from linearity in semilogarithmic plot are more evident and all decays are superimposed. (d) $W_0=10$, here the apparent time scale dependence is inverted, i.e., slopes decrease with t and departure from single-exponential behavior is much more evident.

tered at $W_0=10$ ($\beta=1/4$) for $t\leqslant t^*$, whereas above t^* the linear relationship is restored. As a whole, these results clearly demonstrate that the transition from super- to subdiffusive regime occurs smoothly by crossing an intermediate apparent Gaussian behavior.

B. Oil dilution line, $\Phi=0.02-0.05$ at fixed $W_0=4$

An analogous series of self-diffusion experiments has also been carried out by varying the micellar volume fraction Φ in the range 0.02–0.05, while keeping constant $W_0=4$. The semilogarithmic plots of the experimental surfactant echo decays vs q^2t are shown in Fig. 3.

A slight different situation occurs, here, in comparison to the previous water dilution line. Indeed, when the time dependence of echo decays is checked by varying the surfactant concentration (at fixed W_0) instead of water content, we observe time-dependent echo attenuations in the whole time window explored, $t=20-800$ ms, for $\Phi=0.02$ [Fig. 3(a)], but at higher Φ the temporal dependence disappears as it is evident in Figs. 3(c) and 3(d). Moreover, in the correspondence of $\Phi=0.03$ [Fig. 3(b)], a superdiffusive behavior, characterized by an increment of initial slope of measured $E(q,t)$,

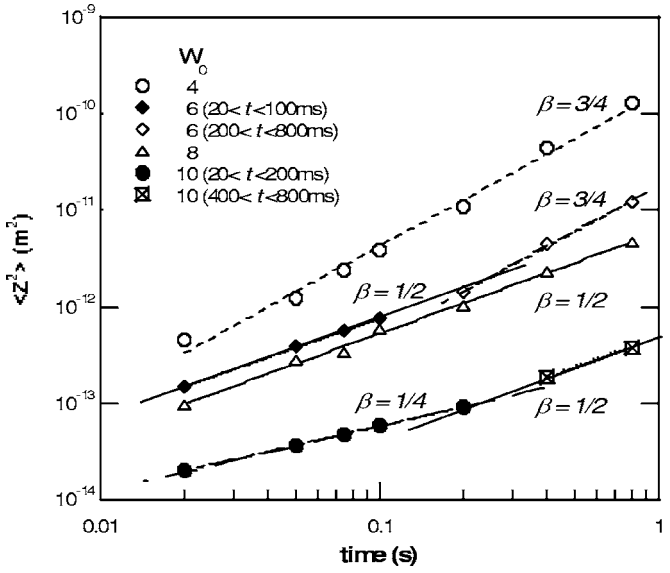

FIG. 2. Log-log plot of surfactant mean square displacement $\langle z^2 \rangle$ as a function of experimental diffusion time t at different water to lecithin molar ratio, $W_0=4-10$ and constant micellar (lecithin *plus* water) volume fractions, $\Phi=0.02$. Lines represent least-squares fits according to the power law described in Eq. (6): dashed is super diffusion ($\beta>1/2$), solid is normal diffusion ($\beta=1/2$), and long-dashed is subdiffusion ($\beta<1/2$). Calculated scaling exponents β are also displayed for each W_0.

with increasing time scale, is encountered for $t>t^*$, where t^* is approximately 100 ms. In the present series as well, all attenuations are always far from pure exponential behavior. As before, the related MSD time dependence has been checked to study the scaling parameter β along the oil dilution line and the results displayed in Fig. 4. Here, we can observe the superdiffusive scaling $\beta=\frac{3}{4}$ at the lowest Φ, which is also correspondent to the highest values of calculated $\langle z^2 \rangle$. At higher concentrations, β decreases toward $\frac{1}{2}$ and only for $t<t^*$ at $\Phi=0.03$. Finally, we note that the higher the concentration the lower the estimated $\langle z^2 \rangle$ is.

V. DISCUSSION

Transport processes characterized by a MSD, $\langle z^2(t) \rangle \sim t^{2\beta}$, which deviates from linear time dependence $(\beta=\frac{1}{2})$ typical of classical Brownian motion are called anomalous. Subdiffusion corresponds to $0<\beta<1/2$ while superdiffusion is characterized by $\frac{1}{2}<\beta<1$. There have been many attempts to model anomalous diffusion by means of generalized diffusion equations in order to provide a mathematical description of the process [33–38]. In what follows, we describe the experimental results in terms of fractional diffusion equations (see Ref. [34] for a comprehensive review on this topic of mathematical physics). Such an approach presents the advantage of using the same treatment for sub- and superdiffusion. Indeed, as the subdiffusion is described as a random walk with memory, analogously the superdiffusion can be thought as a ballistic motion with memory.

A. Large micelles. Subdiffusive regime $\langle z^2(t) \rangle \sim t^{1/2}$

The lecithin MSD in samples at $W_0=10$ and $\Phi=0.02$ scales as the square root of t for time scale below 200 ms (Fig. 2). For higher Φ values the relation $\langle z^2 \rangle \sim \sqrt{t}$ holds up to $t=1.5$ s (see Ref. [15]). At this water-to-lecithin ratio, reverse micelles have cylindrical shape and are extremely long so that samples are viscoelastic [39]. By comparing Eq. (12) with the power law of Fig. 2 one deduces $\beta \approx \frac{1}{4}$ at $W_0=10$. As a consequence the echo decay through Eq. (11) becomes

$$E(q,t) = E_{1/2}(x) = e^{x^2} \operatorname{erfc}(x), \tag{13}$$

where $x=q^2 D_{1/2} t^{1/2}$. According to the above equation, the echo attenuations for $\Phi=0.02$ and $W_0=10$ follow the same trend when plotted as a function of $q^2 t^{1/2}$ (see Fig. 5). We note that the $E(q,t)$ in Eq. (13) has the form expected for a random walk on a random walk. Such a kind of motion can be found in the case of polymer segment diffusion in the tube and/or reptation model or in the case of curvilinear surfactant motion along the contour of a polymerlike micelle.

In accordance with Eq. (12) the diffusion constant in the case $2\beta=0.5$ is $D_{1/2}=\langle z^2 \rangle \sqrt{\pi}/4\sqrt{t}$. The MSD of lecithin molecules undergoing lateral diffusion along the contour of a micelle characterized by a persistence length λ is $\lambda(2D_l t)^{1/2}$, where D_l is the curvilinear diffusion coefficient. Thus the x entering Eq. (13) is $x=0.63\lambda q^2 \sqrt{D_l t}$ and Eq. (13) becomes essentially very close to that expected on the basis of its previously derived for lateral diffusion along Gaussian micellar coils [15]. Fit to the data by using Eq. (13) gives the value 1.68×10^{-13} m^2 s$^{-1/2}$ for the fitting parameter $\lambda D_l^{1/2}$. This value is very close to the prevision expected on the base of its concentration dependence $\lambda D_l^{1/2} \sim \Phi^{-0.24}$ calculated for higher lecithin loading in the same micellar system [15].

B. Small micelles. Superdiffusive regime $\langle z^2(t) \rangle \sim t^{3/2}$

In accordance with the dependence of the MSD on t shown in Fig. 2, one obtains $\beta \approx \frac{3}{4}$ for samples at $W_0=4$ and $\Phi=0.02$. At this composition the reverse micelles are expected to be relatively small [39] and the system is just above Φ^*. For $\beta=\frac{3}{4}$, Eq. (12) gives $\langle z^2 \rangle = (8/3\sqrt{\pi})(D_{3/2} t^{3/2})$ and echo decay [Eq. (10)] becomes

$$E(q,t) = E_{3/2}(x) \text{ with } x = q^2 D_{3/2} t^{3/2}. \tag{14}$$

However, the Mittag-Leffler function cannot be expressed in terms of elemental functions for $\beta=\frac{3}{4}$ and has to be evaluated numerically. First, Eq. (11) has been calculated through a suitable subroutine by which a finite number of terms in the sum is chosen automatically for a wanted precision. In this case the parameter $D_{3/2}$ has been estimated iteratively. Then, the coefficient has been refined through a subsequent global fitting algorithm by using the experimental data $E(q,t)$ for the sample $\Phi=0.02$ and $W_0=4$, collected in the time scale 20–800 ms. These data plotted vs the new abscissa $q^2 t^{3/2}$ fall on the same master curve and the time dependence found in the conventional Stejskal-Tanner plot of Fig. 1(a) disappears. That this is indeed the case is shown in Fig. 6, where the plot of the best fit of Eq. (11) to the data is displayed as well, giving rise to a calculated fitting parameter $D_{3/2}=6.5 \times 10^{-11}$ m^2 s$^{-3/2}$. A similar good agreement was also found for $W_0=6$ in the time window above t^*.

In our polymerlike micellar system, at volume fractions very close to the crossover from the dilute to semidilute re-

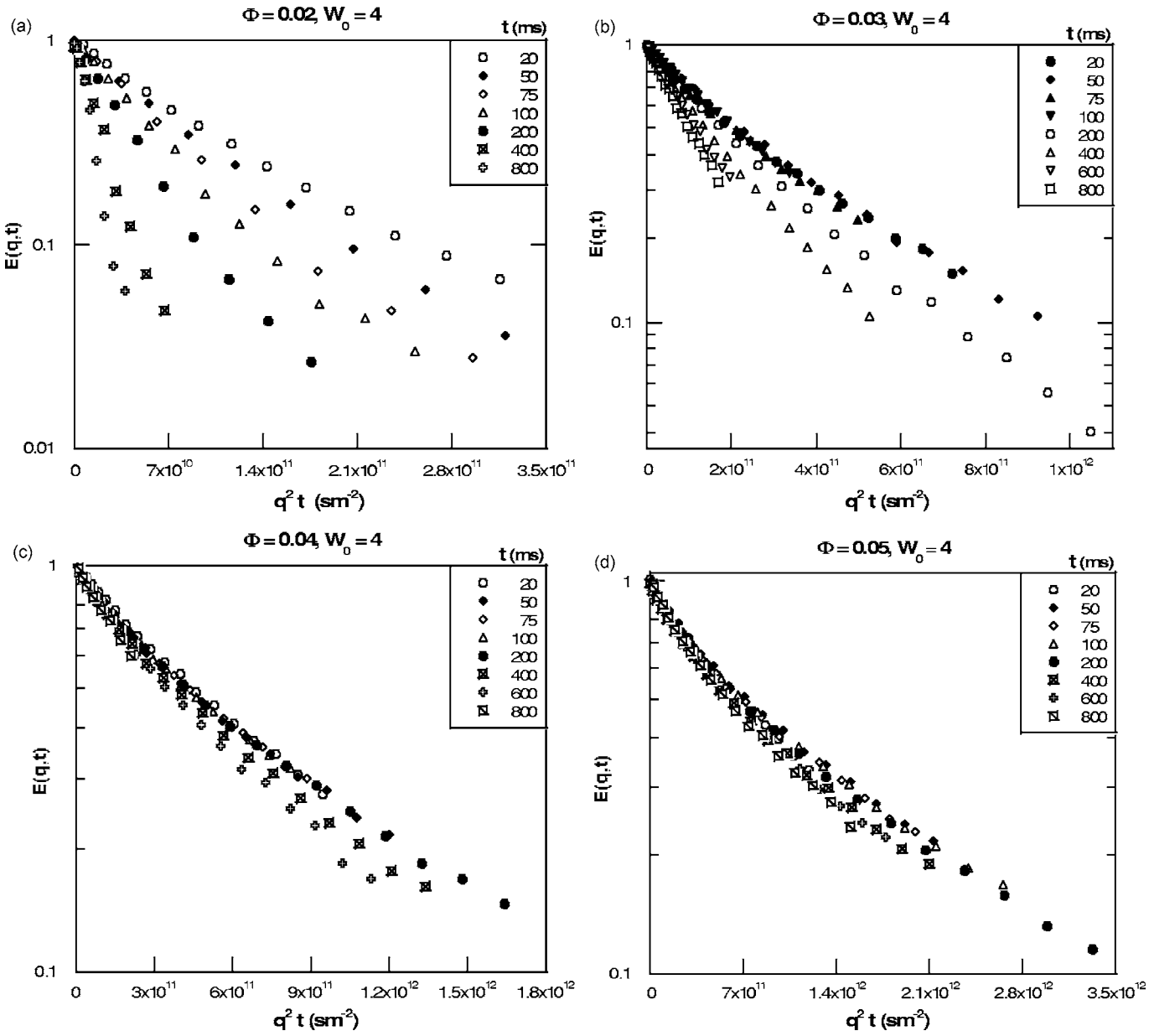

FIG. 3. Semilogarithmic plots of normalized lecithin echo attenuations $E(q,t)$ for $t=20-800$ ms, as a function of q^2t at different micellar volume fractions $\Phi=0.02-0.05$ and constant water to lecithin molar ratio $W_0=4$. (a) $\Phi=0.02$ [same plot reported in Fig. 1(a) displayed also here for clarity]; (b) $\Phi=0.03$, here echoes overlap in the time window $20<t<100$ ms while at higher t slopes increase with time t indicating superdiffusive behavior; (c) $\Phi=0.04$, deviations from linearity in semilogarithmic plot are more evident and most of decays are superimposed. (d) $\Phi=0.05$, all decays overlap in the whole t and deviations from exponentiality is much more evident.

gime, a coexistence of small reverse micelles with extended network fragments (fractal entities) is expected due to the intrinsic broad size polydispersity typical of living polymers. This point provides hints for a possible physical interpretation of the superdiffusive behavior observed close to Φ^*. When Φ^* is approached, giant wormlike micelles become stuck for a time scale short enough, while small micelles may still diffuse by crossing the network meshes. Isliker and Vlahos [40] treated the random walk problem of particles traveling freely through a fractal environment which can be scattered off into random directions when they hit the fractal. For simulated fractal models they predicted enhanced diffusion for random walkers if the dimension of the fractal is less than two, giving rise asymptotically to a pure ballistic behavior. The order of fractional time derivative 2β in Eq. (7) is related to the dynamic fractal dimension d_w through $\beta=d_w^{-1}$ [41], which in turn means that Eq. (12) predicts $d_w=4/3<2$. With slightly increasing W_0 or Φ, the system moves deeper into the semidilute regime and the motion of all the micelles is severely hindered. It is only for longer observation times (above the critical time t^*) that the diffusion of the smallest micelles becomes discernible again giving rise to an enhanced diffusion. At the opposite limit (high W_0 and/or Φ) the semidilute network of extremely long micelles is fully

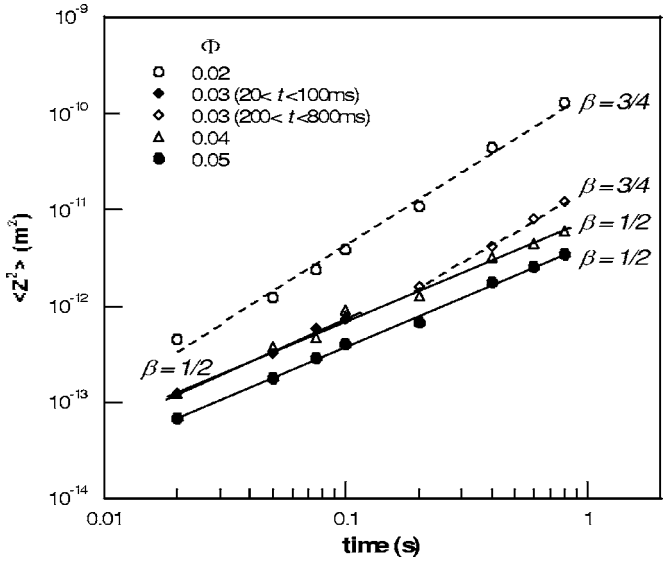

FIG. 4. Log-log plot of lecithin mean square displacement $\langle z^2 \rangle$ as a function of experimental diffusion time t at different micellar volume fractions Φ and constant water to lecithin molar ratio, $W_0=4$. Lines represent least-squares fits according to the power law described in Eq. (6). Calculated scaling exponents β are displayed for each volume fraction.

jammed (over the time scale accessible to PGSE NMR) and the main mechanism for surfactant motion is the lateral diffusion along the contour of immobile micelles. According to such a scenario, the $\beta=\frac{1}{2}$ regime found at intermediate time scale and composition should be due to a compensation between super- and subdiffusional behavior instead of a true Gaussian process. The nonexponential decays of Figs. 1(c) and 3(d) support such an interpretation.

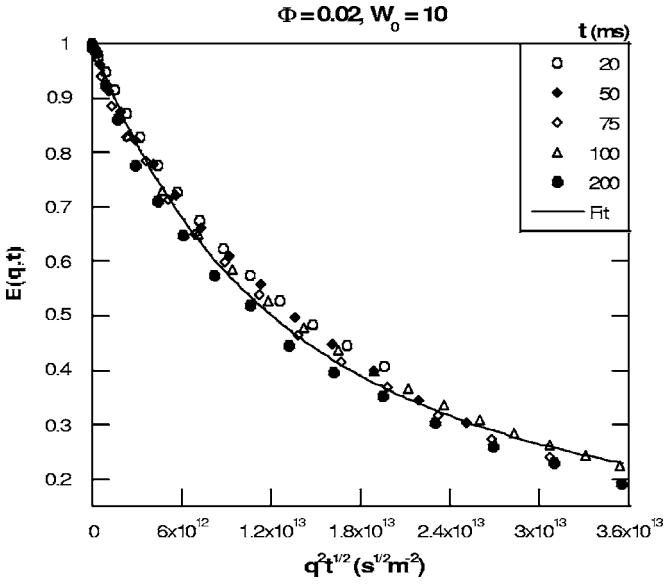

FIG. 5. Normalized surfactant echo attenuations $E(q,t)$ measured in the time window 20–200 ms, from $\Phi=0.02$ and $W_0=10$, as a function of $q^2t^{1/2}$. The solid line is the least-squares global fit of Eq. (13), giving the value 1.68×10^{-13} m^2 s$^{-1/2}$ for the fitting parameter $\lambda D_l^{1/2}$.

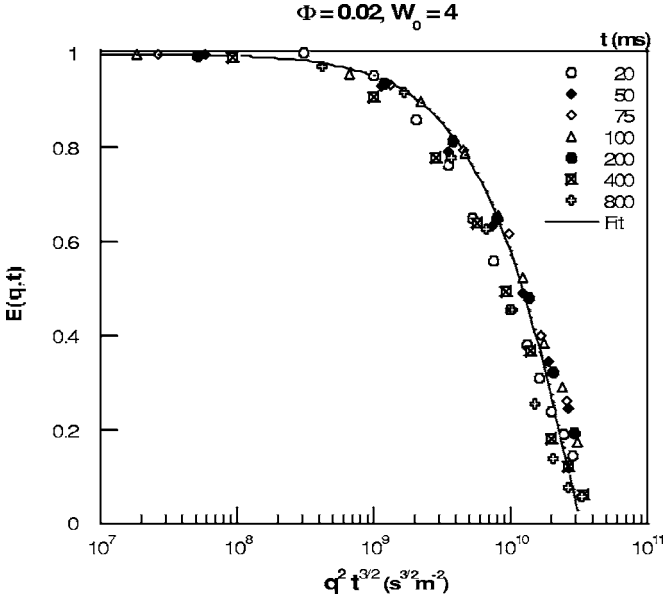

FIG. 6. Normalized surfactant echo attenuations $E(q,t)$ from $\Phi=0.02$ and $W_0=4$, as a function of $q^2t^{3/2}$ in semilogarithmic plot. The solid line is the least-squares global fit of Eq. (11), giving the value 6.5×10^{-11} m^2 s$^{-3/2}$ for the fitting parameter $D_{3/2}$. Symbols have same meaning as in Fig. 1(a) and 3(a).

Continuous transitions from super- to normal to subdiffusion have been identified for surfactant diffusion measured through NMR PGSE technique, in a series of samples where Φ was kept constant and W_0 increased from four to ten. At variance, only a super- to normal transition could be observed along an oil dilution path with constant $W_0=4$. For the investigated micellar system we can sum up the following results: we have found an experimental fingerprint of superdiffusion for compositions very close to the overlap concentration of lecithin wormlike micelles, whose contour length covers a very broad size distribution. A superdiffusive behavior was also observed experimentally in two other surfactant systems: (i) in highly concentrated spherical reverse micelles made up with a phospholipid mixture (asolectin) investigated by means of PGSE NMR [16]; (ii) in direct wormlike micelles investigated by means of fluorescence recovery after photobleaching [13,14]. In both these studies the superdiffusion has been rationalized in terms of Levy's flight under the *ad hoc* ansatz of surfactant exchange dynamics. Here we have interpreted the observed power law dependence of MSD in terms of a scaling parameter according to mathematical description of the diffusion equation developed in terms of *fractional* derivatives. The water-induced micellar growth was very well probed by self-diffusion measurements along the explored water dilution line [Figs. 1(a)–1(d) and Fig. 2], where we have been able to monitor a continuous transition superdiffusion $\rightarrow$ Gaussian $\rightarrow$ subdiffusion along the series $W_0=4\rightarrow10$ at $\Phi=0.02$.

Finally, we note that both classical [Eq. (3)] and fractional diffusion [Eq. (7)] equations furnish only a phenomenological description of the motion. In order to have insight into the molecular mechanism, one has to tailor a suitable model

for the displacement of the spin-bearing molecules. This has been done for the subdiffusion regime (that was interpreted in terms of lecithin lateral diffusion along the micelle contour) while the case of superdiffusion remains to be fully understood. We suggest that the proposed approach can be used to interpret NMR self-diffusion data obtained whenever the complexity of micellar systems may give rise to these extremely peculiar anomalous diffusion phenomena.

ACKNOWLEDGMENTS

This work was supported by the MIUR of Italy (PRIN-COFIN 2003: Nanoscienze per lo Sviluppo di Nuove Tecnologie) and by the Consorzio Interuniversitario per lo sviluppo dei Sistemi a Grande Interfase (CSGI, Firenze). U.O. acknowledges financial support from the Swedish Research Council (VR). We thank Degussa Bioactives AG for lecithin.

[1] G. M. Viswanathan, V. Afanasyef, S. V. Buldyrev, E. J. Murphy, P. A. Prince, and H. E. Stanley, Nature (London) **381**, 413 (1996).
[2] S. V. Buldyrev, M. Gitterman, S. Havlin, A. Ya. Kazakov, M. G. E. da Luz, E. P. Raposo, H. E. Stanley, and G. M. Viswanathan, Physica A **302**, 148 (2001).
[3] G. M. Viswanathan, V. Afanasyef, S. V. Buldyrev, S. Havlin, M. G. E. da Luz, E. P. Raposo, and H. E. Stanley, Physica A **295**, 85 (2001).
[4] R. N. Mantegna and H. E. Stanley, *An Introduction to Econophysics* (Cambridge University Press, Cambridge, England, 1999).
[5] R. N. Mantegna and H. E. Stanley, Nature (London) **383**, 587 (1996).
[6] M. Shlesinger, B. West, and J. Klafter, Phys. Rev. Lett. **58**, 1100 (1987).
[7] J. Klafter, M. F. Shlesinger, and G. Zumofen, Phys. Today **49**, 33 (1996).
[8] E. R. Weeks, J. S. Urbach, and H. L. Swinney, Physica D **97**, 291 (1996).
[9] G. Zumofen, J. Klafter, and M. Shlesinger, Phys. Rev. Lett. **77**, 2830 (1996).
[10] A. Ott, J. P. Bouchard, D. Langevin, and W. Urbach, Phys. Rev. Lett. **65**, 2201 (1994).
[11] O. V. Bychuk and B. O'Shaughnessy, Phys. Rev. Lett. **74**, 1795 (1994).
[12] I. M. Sokolov, J. Mai, and A. Blumen, Phys. Rev. Lett. **79**, 857 (1997).
[13] J. P. Bouchaud, A. Ott, D. Langevin, and W. Urbach, J. Phys. II **1**, 1465 (1991).
[14] A. Ott, J. P. Bouchaud, D. Langevin, and W. Urbach, Phys. Rev. Lett. **65**, 2201 (1990).
[15] R. Angelico, U. Olsson, G. Palazzo, and A. Ceglie, Phys. Rev. Lett. **81**, 2823 (1998).
[16] G. Wolf and E. Kleinpeter, Langmuir **21**, 6742 (2005).
[17] R. Angelico, A. Ceglie, U. Olsson, and G. Palazzo, in *Self-Assembly*, edited by B. H. Robinson (IOS Press, Burke, VA, 2003), p. 318 and references therein.
[18] P. Schurtenberger and C. Cavaco, Langmuir **10**, 100 (1994).
[19] R. Angelico, A. Ceglie, U. Olsson, and G. Palazzo, Langmuir **16**, 2124 (2000).
[20] M. E. Cates and S. J. Candau, J. Phys.: Condens. Matter **2**, 6869 (1990).
[21] K. Shinoda, M. Araki, A. S. Sadaghiani, A. Khan, and B. Lindman, J. Phys. Chem. **95**, 989 (1991).
[22] B. Lindman, U. Olsson, and O. Söderman, in *Handbook of Microemulsion Science and Technology*, edited by P. Kumar and K. L. Mittal (Marcel Dekker, New York, 1999), Chap. 10.
[23] T. Kato, T. Terao, M. Tsukada, and T. Seimiya, J. Phys. Chem. **97**, 3910 (1993).
[24] P. T. Callaghan, *Principles of Nuclear Magnetic Resonance Microscopy* (Oxford University Press, New York, 1991).
[25] D. J. Tomlinson, Mol. Phys. **25**, 735 (1972).
[26] B. Derrida and Y. Pomeau, Phys. Rev. Lett. **48**, 627 (1982).
[27] J. Bernasconi and W. R. Schneider, J. Phys. A **15**, 729 (1982).
[28] S. Havlin and D. Ben-Avraham, Adv. Phys. **51**, 187 (2002).
[29] E. R. Weeks and H. L. Swinney, Phys. Rev. E **57**, 4915 (1998).
[30] M. Caputo and F. Mainardi, Nuovo Cimento Soc. Ital. Fis., C **1**, 161 (1978).
[31] F. Mainardi, Y. Luchko, and G. Pagnini, Fractional Calculus Appl. Anal. **4**, 153 (2001).
[32] C. Fox, Trans. Am. Math. Soc. **98**, 395 (1961).
[33] D. A. Benson, S. W. Wheatcraft, and M. Meerschaert, Water Resour. Res. **36**, 1413 (2000).
[34] R. Metzler and J. Klafter, Phys. Rep. **339**, 1 (2000).
[35] E. Barkai and R. J. Silbey, J. Phys. Chem. B **104**, 3866 (2000).
[36] R. Metzler, E. Barkai, and J. Klafter, Phys. Rev. Lett. **82**, 3563 (1999).
[37] G. Zumofen and J. Klafter, J. Chem. Phys. **219**, 303 (1994).
[38] S. Sumiyoshi and S. Thurner, Physica A **356**, 403 (2005).
[39] R. Angelico, B. Balinov, A. Ceglie, U. Olsson, G. Palazzo, and O. Soderman, Langmuir **15**, 1679 (1999).
[40] H. Isliker and L. Vlahos, Phys. Rev. E **67**, 026413 (2003).
[41] T. Zavada, N. Südland, R. Kimmich, and T. F. Nonnenmacher, Phys. Rev. E **60**, 1292 (1999).